Pergamon

Int. J. Heat Mass Transfer. Vol. 40, No. 1, pp. 27–38, 1997

0017-9310/97 $15.00 + 0.00

PII: S0017-9310(96)00087-7

The effects of inlet fluid flow nonuniformity on thermal performance and pressure drops in crossflow plate–fin compact heat exchangers

CH. RANGANAYAKULU,† K. N. SEETHARAMU‡§ and K. V. SREEVATSAN†

†Aircraft Design Bureau, L.C.A. Complex, Hindustan Aeronautics Limited, Bangalore-560 037, India

‡Department of Mechanical Engineering, Indian Institute of Technology, Madras-600 036, India

(*Received* 4 *October* 1995 *and in final form* 27 *February* 1996)

Abstract—An analysis of a crossflow plate–fin compact heat exchanger, accounting for the effects of two-dimensional nonuniform inlet fluid flow distribution on both hot and cold fluid sides, is carried out using a finite element model. A mathematical equation is developed to generate different types of fluid flow maldistribution models considering the possible deviations in fluid flow. Using these fluid flow maldistribution models, the exchanger effectiveness and its deterioration due to flow nonuniformity are calculated for an entire range of design and operating conditions. In addition to thermal analysis, the pressure drops and their variations are also calculated for these models. It was found that the performance deteriorations and variation in pressure drops are quite significant in some typical applications due to fluid flow nonuniformity. Copyright © 1996 Elsevier Science Ltd.

INTRODUCTION

The demand for high performance heat exchange devices having small spacial dimensions is increasing due to their need in applications such as aerospace and automobile vehicles, cooling of electronic equipment and artificial organs [1]. The design theory of compact heat exchangers is based on either the ε-NTU or the log-mean temperature difference concept. In most heat transfer and pressure drop calculations of heat exchangers, it is presumed that the inlet fluid flow distributions across the exchanger core are uniform. This assumption is generally not realistic under actual operating conditions due to space limitations, especially in aerospace applications. Advancement of the heat exchanger design theory, which takes these effects into consideration, therefore becomes an important project in industry. The flow nonuniformity through the exchanger is generally associated with improper exchanger entrance configuration, due to poor header design and imperfect passage to passage flow distribution in a highly compact heat exchanger caused by various manufacturing tolerances. Passages which are different in size and shape exhibit different flow resistances resulting in a nonuniform flow distribution, even when the flow approaching the core face is uniform. The maldistributions are also caused by the heat transfer process itself, i.e. viscous flow coolers or thermoacoustic oscillations, two-phase flows which are very difficult to distribute uniformly and fouling and/or corrosion which can affect the flow distribution. Also, constant heat property assumptions leading to a constant heat transfer coefficient (hereinafter called CHTC) are used in heat exchanger design. Fluid properties vary along the flow direction, especially when the temperature difference is large. Hence, it is necessary to consider its effect on the thermal performance of the heat exchanger.

The flow maldistribution effects have been well recognized and presented [3–15] for heat exchangers and cooling towers. Previous works [3–6, 8, 9, 12] are either limited to the studies of the deterioration of exchanger performance due to one-dimensional flow nonuniformity or to two-dimensional flow nonuniformity on any one fluid side. There are cases when the flow maldistributions are two-dimensional across the exchanger cores and can occur on both fluid sides. Investigation of the deterioration of exchanger performance due to two-dimensional flow nonuniformity on both fluid sides is very limited [7]. All of them have neglected the effect of fluid property variations, while investigating the flow nonuniformity effects. However, Ravikumar *et al.* [16, 17] and Yamasheta *et al.* [18] have developed a numerical procedure based on the finite element method to analyse the performance of crossflow compact heat exchangers without considering the flow nonuniformity effects. Moreover, all the previous works [3–6, 8, 9, 12, 13] were limited to specific types of nonuniform flow models and cannot be interpolated or extrapolated for other types of flow maldistributions. No generalized solutions are available for interpolation/extrapolation of

§Author to whom correspondence should be addressed.

NOMENCLATURE

A heat transfer area [m^2]
a elemental length of the exchanger in the x-direction [m]
b elemental length of the exchanger in the y-direction [m]
c_p specific heat of the fluid at constant pressure [J kg^{-1} K^{-1}]
C Mc_p = fluid heat capacity rate [J s^{-2} K^{-1}]
CHTC constant heat transfer coefficient case
D pressure gradient constant in equations (1)–(4)
d width of the exchanger inlet duct [m]
f local friction factor
G flow stream mass velocity [kg s^{-1} m^{-2}]
g proportionality factor in Newton's second law
h convection heat transfer coefficient [W m^{-2} K^{-1}]
I divisions in the x-direction $(1, 2, 3 \ldots n)$
J divisions in the y-direction $(1, 2, 3 \ldots n)$
k thermal conductivity of the exchanger wall [W m^{-1} K^{-1}]
L length of exchanger transition duct/header [m]
M mass flow rate [kg s^{-1}]
n number of divisions
NTU AU/C_{min} = number of transfer units, dimensionless
p pressure gradient constant in equations (1)–(4)
Q enthalpy/heat entering or leaving the plate [W]
S total heat transfer area [m^2]
S_f minimum free flow area [m^2]
T temperature of hot/cold fluids and metal wall [°C]
U overall heat transfer coefficient [W m^{-2} K^{-1}]
V_1, V_2 specific volumes of inlet and outlet fluids [m^3 kg^{-1}]
V_m mean specific volume [m^3 kg^{-1}]
VTHC variable heat transfer coefficient case
x coordinate in the x-direction [m]
y coordinate in the y-direction [m]
z coordinate in the z-direction [m].

Greek symbols

α flow nonuniformity parameter defined in equation (5)
β a constant such as $h = f(G^\beta)$
ε exchanger effectiveness $= \dfrac{C_h(T_{h,i} - T_{h,o})}{C_{min}(T_{h,i} - T_{c,i})} = \dfrac{C_c(T_{c,o} - T_{c,i})}{C_{min}(T_{h,i} - T_{c,i})}$
μ constant in equation (1)
ϕ constant in equation (1)
τ flow nonuniformity effect factor as defined in equation (16)
σ ratio of free flow area to frontal area
θ overall surface efficiency, dimensionless.

Subscripts

c cold side
b bottom plate
h hot side
i inlet
m middle plate
max maximum magnitude
min minimum magnitude
o outlet
t top plate
1–7 node numbers when T or Q is used.

results for possible flow maldistributions due to inlet poor header design, called gross flow maldistribution. Also, no analysis is available as quoted by Shah [8] for pressure drop variations due to gross flow maldistribution. Since, such nonuniform flow is associated with poor header design, the static pressure distributions at the core inlet and outlet faces may not be uniform.

The objective of the thermal design of a heat exchanger is to determine the most favourable size and configuration of the exchanger core, which meets the demand of the required heat transfer rate within the specified fluid pressure drops, space and cost limitations. Hence, the present analysis has been carried out to determine the effects of gross flow maldistribution of the crossflow heat exchanger on thermal performance and pressure drop variations for two cases: flow nonuniformity on only one side and flow nonuniformity on both sides of the subject heat exchanger. In each case, three different magnitudes of two-dimensional velocity profiles are considered at the core entrance in this analysis.

The design of the headers and inlet ducts significantly affects the velocity distribution approaching the face of the exchanger core, as shown in Fig. 1(a). In this type of flow maldistribution, the variations in flow at the inlet of the exchanger core mainly depend on the location of the inlet duct, the ratio of core frontal area ($2a \times 3b$) to inlet duct cross-sectional area (d^2), the distance of transition duct/header (L)

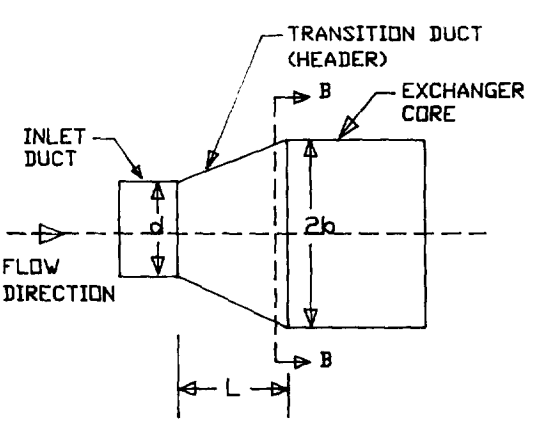

(a) EXCHANGER SCHEMATIC

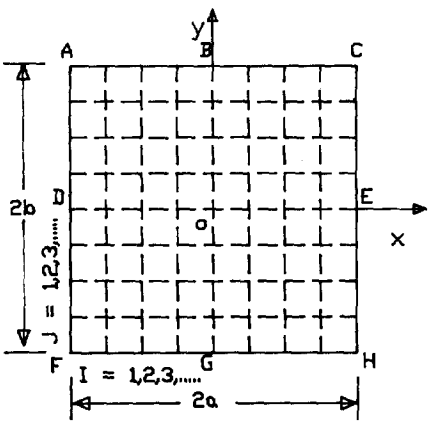

(b) EXCHANGER CORE FRONTAL FACE
(Sectional view - BB)

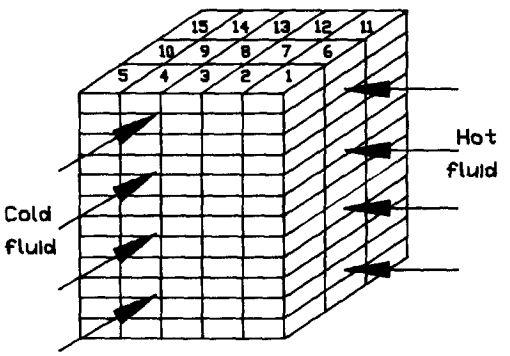

(c) DISCRETISED EXCHANGER

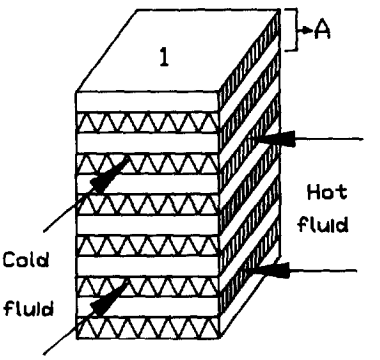

(d) A STRIP [1]

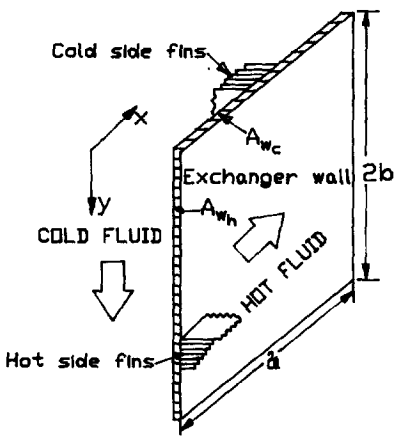

(e) EXCHANGER WALL WITH FINS

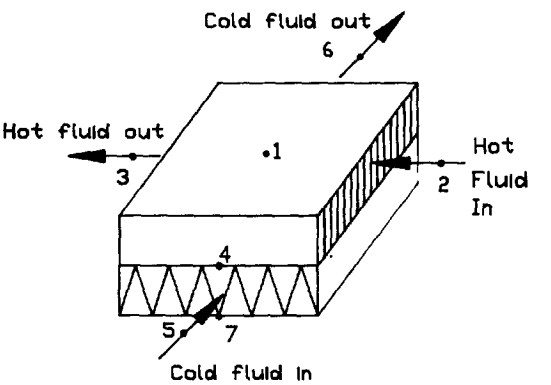

(f) AN ELEMENT STACK [A]

Fig. 1. Crossflow compact plate–fin heat exchangers: (a) an exchanger schematic; (b) an exchanger frontal face; (c) a discretized exchanger; (d) a strip I; (e) exchanger wall with fins; (f) an element stack.

between the core face and inlet duct and the shape of headers, i.e. oblique flow headers or normal flow headers and with/without manifolds. These velocity profiles are either one-dimensional or two-dimensional and either linear or nonlinear depending on the flow pattern as discussed. In these cases, generally, the pressure gradient is often higher at the centre than that at the edge of the exchanger core.

MATHEMATICAL EQUATIONS

Based on the concept of Fourier series, a mathematical equation is developed to generate the flow nonuniformity models at the exchanger inlet (either hot fluid side or cold fluid side). The heat exchanger core frontal face is a rectangular domain having edges $2a$ and $2b$ in the x–y plane as shown in Fig. 1(b) and will be a square domain when $a = b$. The lengths with respect to origin o are $x = a$ or $x = -a$ and $y = b$ or $y = -b$.

The cold fluid flows under the influence of a constant pressure gradient in the z-direction and its equation is

$$\frac{\partial^2 W_c}{\partial x^2} + \frac{\partial^2 W_c}{\partial y^2} = \frac{\partial P_c}{\mu \partial z} = \text{a constant.} \qquad (1a)$$

The same equation can be used for other fluids, provided the x-, y- and z-coordinates are changed accordingly. Similarly, the hot fluid flows under the influence of a constant pressure gradient in the x-direction and its equation is

$$\frac{\partial^2 W_h}{\partial y^2} + \frac{\partial^2 W_h}{\partial z^2} = \frac{\partial P_h}{\mu \partial x} = \text{a constant.} \qquad (1b)$$

We feel that only one equation can be shown by removing the subscript c or h in the above equations (1a) and (1b) to avoid repeating the equations. Then the equation for the fluid (cold or hot fluid) at the exchanger inlet duct can be represented as

$$\frac{\partial^2 W}{\partial x^2} + \frac{\partial^2 W}{\partial y^2} = \frac{\partial P}{\mu \partial z} = \text{a constant.} \qquad (1c)$$

On the boundary,

$$\text{at } x = +/-a, w(+/-a, y) = 0 \qquad (2)$$

$$\text{at } y = +/-b, w(x, +/-b) = 0. \qquad (3)$$

The term $\partial P/\mu \partial z$ can be regarded as a known constant, since the choice of the pressure gradient is in one's control here. As such there is only one unknown, *viz.* $W = W(x, y)$ controlled by equations (1)–(3) above. The solution to represent the fluid velocity (W) is

$$W(x,y) = \frac{64D}{\pi^4} \sum_{m,n=0}^{\infty} \times \left[\frac{(-1)^{m+n+1}}{\left[\left(\frac{2m+1}{a}\right)^2 + \left(\frac{2n+1}{b}\right)^2\right](2m+1)(2n+1)} \cos\frac{(2m+1)\pi x}{2a} \cos\frac{(2n+1)\pi y}{2b} \right]. \qquad (4)$$

Also, the local flow nonuniformity parameter (α) is defined as [4]

$$\alpha = \frac{\text{actual local mass flow rate}}{\text{average mass flow rate if the fluid flow is uniform}}. \qquad (5)$$

Equation (4) is used to calculate the actual local mass flow rates at the entry of the exchanger duct by assuming a constant pressure gradient. However, the nondimensional flow nonuniformity parameter (α) is more useful for relative comparison. Using the above equations, one type of nondimensional flow nonuniformity model is generated, which is independent of pressure gradient, considering the average mass flow rate as unity. This model is shown as A0 in Table 1. In order to produce three more flow nonuniformity models, the velocity profile has been distorted, however, keeping the average mass flow rate as unity. These models are shown as A1, A2 and A3 in Table 1. The nonzero velocity values in the proposed models are at the points away from the wall of transition duct. In each model, there are 10×10 local flow nonuniformity dimensionless parameters (αs), which correspond to the 10×10 subdivisions on the x–y plane perpendicular to the direction of the nonuniform fluid flow. In view of the symmetry of the velocity profiles (which have been used for convenience) only one-fourth of αs are presented in Table 1.

FINITE ELEMENT ANALYSIS

A discretized model of a crossflow heat exchanger is shown in Fig. 1(c). It is divided into a number of equal strips.

The strip 1 is isolated and shown in Fig. 1(d). The subject exchanger may be visualized as a wall separating the two fluid streams flowing at right angles and with plate–fins on both sides as shown in Fig. 1(e). Each strip consists of a number of pairs of seven-noded stacks which carry hot and cold fluids as shown in Fig. 1(f). These are the basic elemental exchangers for which the finite element equations are formulated using Galerkin's method [19]. The linear elements (two-noded) for both hot and cold fluids are considered in the present analysis. The following assumptions are made in this analysis:

(1) the thickness of the exchanger wall is small as compared to its other two dimensions, so that the thermal resistance through the exchanger wall in the direction normal to the fluid flows is small enough to be neglected;

(2) no phase change and no heat generation within the exchanger;

(3) fluids other than liquid metals are considered—their temperatures remain constant and uniform over their respective inlet sections;

Table 1. Four flow maldistribution models

$I=$	1;10	2;9	3;8	4;7	5;6
			Model A0		
$J=1;10$	0.000	0.000	0.000	0.000	0.000
2;9	0.000	0.282	0.554	0.800	0.996
3;8	0.000	0.554	1.089	1.579	1.975
4;7	0.000	0.800	1.579	2.305	2.903
5;6	0.000	0.996	1.975	2.903	3.702
			Model A1		
$J=1;10$	0.100	0.100	0.100	0.100	0.100
2;9	0.100	0.352	0.597	0.819	0.996
3;8	0.100	0.597	1.080	1.523	1.879
4;7	0.100	0.819	1.523	2.177	2.717
5;6	0.100	0.996	1.879	2.717	3.438
			Model A2		
$J=1;10$	0.500	0.500	0.500	0.500	0.500
2;9	0.500	0.639	0.776	0.899	0.998
3;8	0.500	0.776	1.045	1.291	1.489
4;7	0.500	0.899	1.291	1.655	1.956
5;6	0.500	0.998	1.489	1.956	2.356
			Model A3		
$J=1;10$	0.900	0.900	0.900	0.900	0.900
2;9	0.900	0.923	0.952	0.978	0.999
3;8	0.900	0.952	1.009	1.062	1.104
4;7	0.900	0.978	1.062	1.139	1.203
5;6	0.900	0.999	1.104	1.203	1.289

(4) the exchanger where both of the fluids are unmixed is considered—cross or transverse mixing of fluids is not considered;

(5) the heat transfer surface configurations and the heat transfer areas on both sides per unit base area are constant and uniform throughout the exchanger;

(6) in the elements, the temperatures of the fluid are assumed to vary only along their flow lengths;

(7) the entry length effects are not considered in the present analysis;

(8) steady-state conditions are assumed;

(9) axial heat conduction in either of the fluids and in the exchanger wall is neglected in this analysis;

(10) the convection heat transfer coefficient between the fluids and their respective heat transfer surfaces is directly proportional to the mass velocity of the fluid flow or $h = f(G^{\beta})$.

Based on the above assumptions, the governing energy balance equations for nonuniform fluid flow in the exchanger core are

$$(\theta hA)_h(T_h - T_{w,t}) = Q_t \tag{6}$$

$$-\alpha(Mc_p)_h\frac{\partial T_h}{\partial x} + \frac{(\theta hA)_h}{a}(T_h - T_{w,t}) + \frac{(\theta hA)_h}{a}(T_h - T_{w,m}) = 0 \tag{7}$$

$$(\theta hA)_h(T_h - T_{w,m}) - (\theta hA)_c(T_{w,m} - T_c) = 0 \tag{8}$$

$$\alpha(Mc_p)_c\frac{\partial T_c}{\partial y} + \frac{(\theta hA)_c}{b}(T_{w,m} - T_c) + \frac{(\theta hA)_c}{b}(T_{w,b} - T_c) = 0 \tag{9}$$

$$(\theta hA)_c(T_{w,b} - T_c) = Q_b \tag{10}$$

and the boundary conditions are

$$T_h(0, y) = T_{h,in}; \quad T_c(x, 0) = T_{c,in}. \tag{11}$$

The temperatures of the cold (T_c) and hot (T_h) fluids in the element are approximated by a linear variation as

$$T_h = N_i T_{h,2} + N_j T_{h,3} \tag{12}$$

$$T_c = N_k T_{c,5} + N_l T_{c,6}, \tag{13}$$

where N_i, N_j, N_k and N_l are shape functions, $N_i = 1 - x/a$, $N_j = x/a$ for a cold fluid and $N_k = 1 - y/b$, $N_l = y/b$ for a hot fluid. The boundary conditions to be satisfied are

$$(\alpha Mc_p)_h T_{h,2} = Q_2 \tag{14}$$

$$(\alpha Mc_p)_c T_{c,5} = Q_5. \tag{15}$$

Substituting the approximations (12) and (13) into equations (6)–(10) and applying the subdomain collocation procedure to minimize the error over the entire domain, the final set element matrices can be obtained as [16]

$$\begin{bmatrix} j_h & -j_h/2 & -j_h/2 & 0 & 0 & 0 & 0 \\ 0 & i_h & 0 & 0 & 0 & 0 & 0 \\ j_h & -i_h-j_h & -j_h+i_h & j_h & 0 & 0 & 0 \\ 0 & -j_h & -j_h & 2(j_h+j_c) & -j_c & -j_c & 0 \\ 0 & 0 & 0 & 0 & i_c & 0 & 0 \\ 0 & 0 & 0 & j_h & i_c-j_c & -(i_c+j_c) & j_c \\ 0 & 0 & 0 & 0 & -j_c/2 & -j_c/2 & j_c \end{bmatrix} \times \begin{bmatrix} T_1 \\ T_2 \\ T_3 \\ T_4 \\ T_5 \\ T_6 \\ T_7 \end{bmatrix} = \begin{bmatrix} -Q_t \\ Q_2 \\ 0 \\ 0 \\ Q_5 \\ 0 \\ Q_b \end{bmatrix},$$

where $j_h = (\theta hA)_h$, $i_h = (\alpha Mc_p)_h$, $j_c = (\theta hA)_c$ and $i_c = (\alpha Mc_p)_c$.

The element matrices for other pairs of stacks in the strip [Fig. 1(c)] are evaluated and assembled into a global matrix. The term Q_b on the right-hand side of the matrix gets cancelled when the adjacent element is assembled. It remains on the right-hand side of the global matrix only for the bottom pair of stacks. Similarly, Q_t remains only for the top pair of stacks. If the top and bottom surfaces are insulated, then Q_t for top pair of stacks and Q_b for the bottom pair become zero. The final sets of simultaneous equations are solved after incorporating the known boundary conditions (inlet temperatures) and fluid capacity rates. The outlet temperature of strip 1 [Fig. 1(c)] will be the inlet temperatures for adjacent strips. Thus, by marching in a proper sequence, the temperature distribution in the exchanger is obtained.

The exchanger thermal performance deterioration factor (τ) is introduced as presented by Chiou [3–6] to illustrate the two-dimensional flow nonuniformity on the deterioration of thermal performance. It is defined as

$$\tau = \frac{\varepsilon_{\text{uniform flow}} - \varepsilon_{\text{nonuniform flow}}}{\varepsilon_{\text{uniform flow}}}. \tag{16}$$

The thermal performance deterioration factor (τ) directly shows the degree of deterioration of the exchanger effectiveness. Analytical solutions without considering the effects of flow nonuniformity are obtained using the solution procedure given by Kays and London [2] and others [20, 21]. If the temperatures are not known *a priori*, the iteration is started with assumed outlet temperatures. The new outlet temperatures are calculated and compared with the assumed outlet temperatures. The iterations are continued until the convergence is achieved to the fourth digit for all cases. In the case of CHTC, the fluid properties and heat transfer coefficients are assumed to be constant throughout the exchanger and in the case of uniform flow, the heat capacity rates, $(\alpha Mc_p)_h$ and $(\alpha Mc_p)_c$, are assumed to be constant throughout the exchanger core. In these cases, the heat transfer coefficients are evaluated at the bulk mean temperatures of the fluids. In the case of variable heat transfer coefficient (hereafter called VHTC), the solution procedure to obtain the temperature distribution in the exchanger is similar to that of the CHTC case, except that the heat transfer coefficient and other properties vary from element to element, depending on their local bulk mean temperatures. The temperature distribution on the outlet surfaces of cold and hot fluids are averaged to get the representative outlet mean temperatures for uniform flow cases. In the case of nonuniform flow, the temperature distributions in the elemental heat exchangers on the outlet surfaces are obtained using mass balance, as follows:

mean temperature (T_{mean})

$$= \frac{\alpha_1 M_1 T_1 + \alpha_2 M_2 T_2 + \cdots + \alpha_n M_n T_n}{\alpha_1 M_1 + \alpha_2 M_2 + \cdots + \alpha_n M_n}. \tag{17}$$

In this study, the ranges of the design and operating parameters of the exchanger are as follows:

(1) NTU—1.0–100.0;
(2) C_h/C_c (i.e. $C_{\min}/C_{\max}$)—0.2–1.0;
(3) $(\theta ha)_h/(\theta ha)_c = 1.0$.

STABILITY OF THE METHOD

The accuracy of the solution depends on the number of elements used. Actually, the number of elements used is determined by a compromise between the accuracy desired and the time required by the computer. Use of a greater number of sub-divisions cannot only produce results of higher accuracy, but can also enhance the convergence. A few sample cases, which are of primary interest in the aerospace applications, are considered and tabulated in Table 3 to establish the prediction capability of the method for constant heat transfer cases (CTHC) and variable heat transfer cases (VHTC). A comparison of the results from the present method with the analytical results in Table 4, shows that the present method is capable of predicting accurately the temperature distribution and performance parameters of compact heat exchangers. The error in effectiveness between the CHTC cases and analytical solutions is negligible for most situations. The present finite element analysis results of flow nonuniformity effects have been compared with available results [4] in Fig. 2 for two cases of $C_{\min}/C_{\max} = 1$ and 0.25. This comparison of results is made with the available flow maldistribution models (tabulated in Table 2), taken from previous work [4]. In Fig. 2(a), the percentage deviation between the results of present analysis and available analysis [4] is around 6% for the case of $C_{\min}/C_{\max} = 1$, when compared with thermal performance deterioration

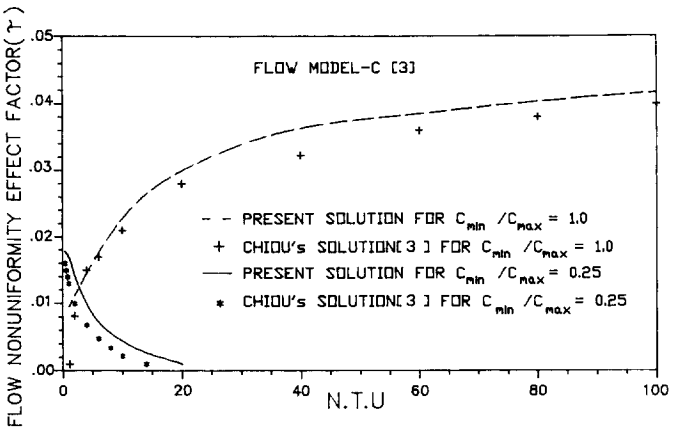

(a) - COMPARISON WITH FLOW NONUNIFORMITY EFFECT FACTOR

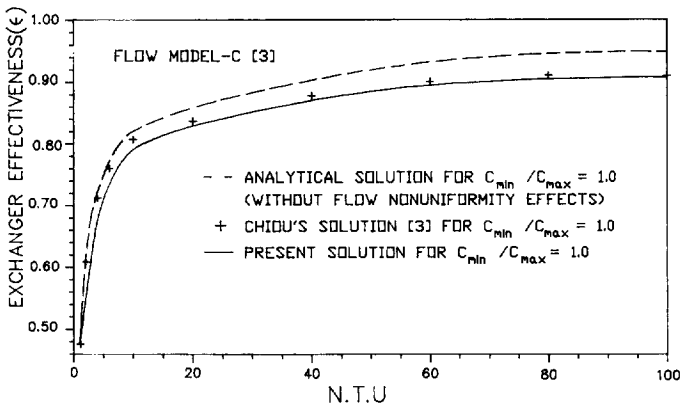

(b) - COMPARISON WITH EXCHANGER EFFECTIVENESS

Fig. 2. Flow nonuniformity effects—comparison of results: (a) comparison with flow nonuniformity effect factor (τ), (b) comparison with exchanger effectiveness (ε).

factor (τ). However, this deviation amounts to only 0.3% when compared with actual effectiveness (ε) values which are more realistic, as shown in Fig. 2(b). This accuracy is believed to be sufficient for most of the engineering applications.

RESULTS AND DISCUSSION

The examples considered earlier for the CHTC case are solved again with the VHTC case and tabulated in Table 3 for an easy comparison of the results. For the same exchanger with similar process entry conditions, in VHTC cases, the ε values are found to be slightly higher, as investigated by Ravikumaur *et al.* [16, 17]. In this analysis, 'air' is used as both cold and hot fluids. It has been observed that the maximum variation in effectiveness is 2% between the CHTC and VHTC cases. In most cases, even a large variation in some physical properties will be reflected only marginally in the performance parameters.

Using the above four typical flow nonuniformity models (shown in Table 1), the thermal performance variations have been calculated for balanced and unbalanced flows of the exchanger. These models are the examples for possible maldistributions when flow inlet ducts are placed at the centre of and in front of the core. The analysis presented in this paper can be applied to linear, transition and turbulent flows if

Table 2. Flow maldistribution model-C [4]

$I=$	1;10	2;9	3;8	4;7	5;6
$J=1;10$	0.720	0.720	0.720	0.720	0.720
2;9	0.720	1.000	1.000	1.000	1.000
3;8	0.720	1.000	1.000	1.000	1.000
4;7	0.720	1.000	1.000	1.500	1.500
5;6	0.720	1.000	1.000	1.500	2.180

Table 3. The effects of fluid property variations

SL. no.	NTU	C_{min}/C_{max}	Exchanger effectiveness (ε)		
			Analytical solution	Finite element analysis CHTC	VHTC
1	2.560	0.946	0.673	0.671	0.670
2	3.815	0.750	0.798	0.795	0.792
3	2.877	1.000	0.681	0.683	0.674
4	2.473	1.000	0.653	0.654	0.655
5	2.326	1.000	0.642	0.643	0.643
6	5.164	0.500	0.898	0.897	0.904
7	8.713	1.000	0.811	0.813	0.816

appropriate βs are used for calculating the convective heat transfer coefficient. It has been observed that the variations in performance deterioration due to flow nonuniformity with $(\theta ha)_h/(\theta ha)_c$ ratio are insignificant, as observed by other investigators [3–5]. Hence, the present analysis has been carried out with $(\theta ha)_h/(\theta ha)_c = 1.0$.

(a) Thermal performance deteriorations due to flow maldistribution

In this paper, the performance evaluation of the effects of flow nonuniformity on a crossflow heat exchanger is presented, for balanced flow, $C_{min}/C_{max} = 1$, as well as for unbalanced flows, C_{min}/C_{max} not equal to one. The exchanger thermal performance deteriorations are plotted as a function of NTU ($NTU_{overall}$) for five magnitudes of $C_{min}/C_{max} = 1.0, 0.80, 0.60, 0.40$ and 0.20 in Figs. 3–7 using Models A0, A1, A2 and A3. In each graph, four different flow nonuniformity models are considered for relative comparison of the results. In each case, the influence of flow nonuniformity on thermal performance is presented for three cases: flow nonuniformity on the minimum fluid capacity (C_{min}) side, flow nonuniformity on the maximum fluid capacity (C_{max}) side and flow nonuniformity on both sides. It must be noted that for any flow model, either flow model can be on the hot or cold fluid side of the exchanger. It can be seen that the exchanger performance deteriorations are quite significant for the A0 and A1 flow models. For example, the maximum ineffectiveness values (at NTU = 100) for flow Model A0 (for flow nonuniformity on C_{min} side) are around 20% for $C_{min}/C_{max} = 1.0$, 17.5% for $C_{min}/C_{max} = 0.8$, 8.5% for $C_{min}/C_{max} = 0.6$, 1.2% for $C_{min}/C_{max} = 0.4$ and 0.012% for $C_{min}/C_{max} = 0.2$. It is noted that when the same flow maldistribution occurs on both fluid sides, the deterioration of the exchanger performance may be lower than those when only one fluid side involves flow maldistribution. Also it has been observed that τ increases as NTU increases in the case of balanced flows, as shown in Fig. 3, whereas τ decreases as NTU increases in the case of unbalanced flows, as shown in Figs. 4–7. In the case of balanced flows, the C_{min} is equal to C_{max} and hence, the performance deterioration values are equal in both cases, as expected, as shown in Fig. 3(a, b). Information presented in these figures is not restricted to models considered in this analysis, but the results can be interpolated for other similar flow models. For example, the results can be interpolated, for any intermediate flow maldistribution model, between the curves, as the upper curve is showing higher performance deviations and the lower curve is showing the minimum performance deviations. The deterioration of thermal performance of a single pass crossflow heat exchanger due to flow nonuniformity presented in Figs. 3–7 is generally similar to those

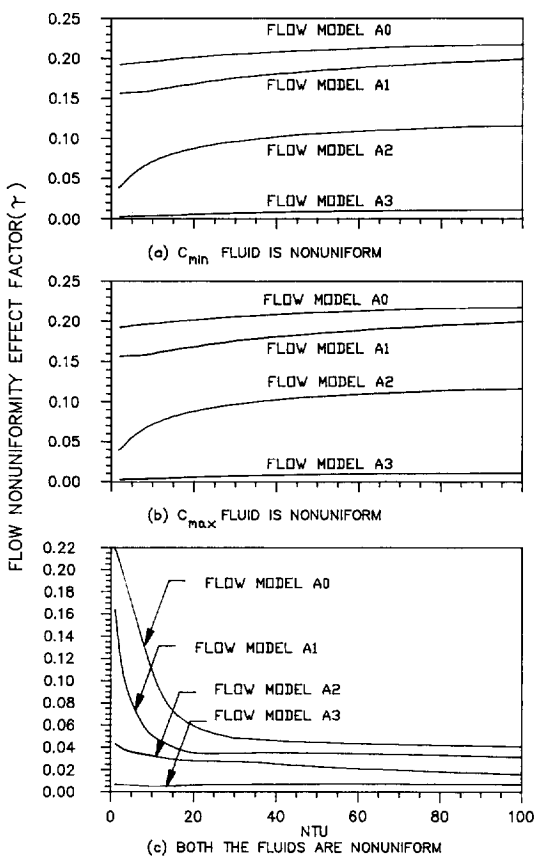

Fig. 3. Flow nonuniformity effects—$C_{min}/C_{max} = 1.0$.

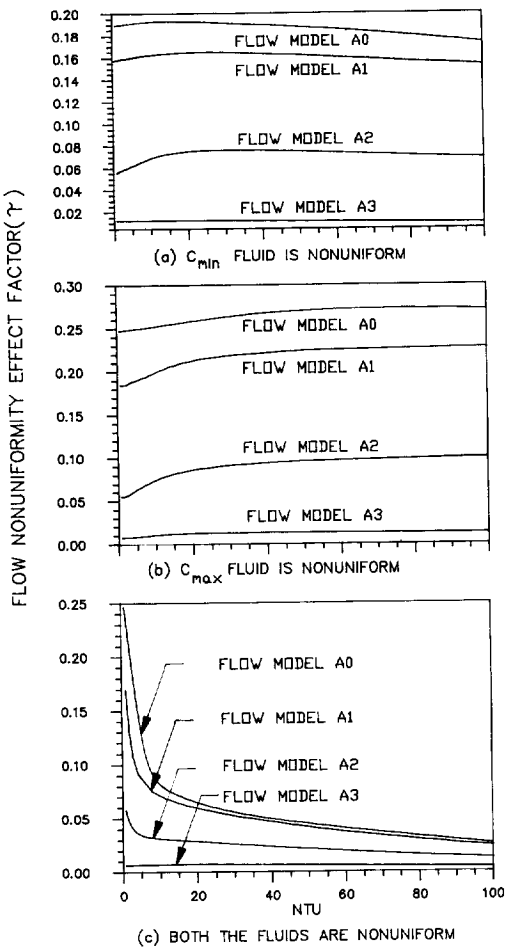

Fig. 4. Flow nonuniformity effects—$C_{min}/C_{max} = 0.8$.

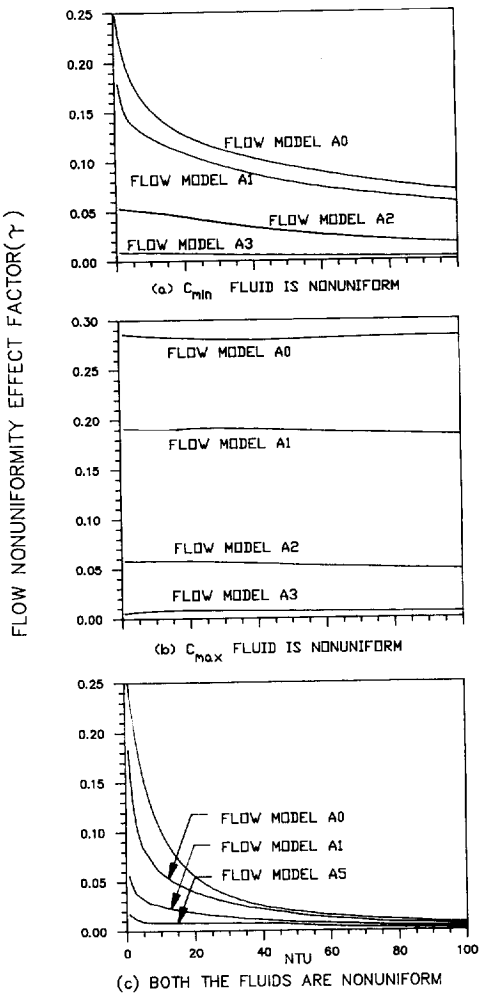

Fig. 5. Flow nonuniformity effects—$C_{min}/C_{max} = 0.6$.

reported in previous investigations [4–9]. However, the type of fluid maldistributions considered in this investigation is basically different from those reported previously; direct comparison of all these results is thus not possible.

(b) Pressure drop variations due to flow maldistribution

The ratio of heat transferred to the pumping power required is an important factor in economizing an exchanger. Pumping power depends upon the pressure drop required to pump the fluid at the required velocity. Hence, it is necessary to estimate the pressure drop along with the thermal performance. The pressure drops in the fluids are evaluated using the following formula [2]:

$$\text{pressure drop } (\Delta_P) = \frac{G^2 V_i}{2g} \times \left[(1+\sigma^2)\left(\frac{V_2}{V_1} - 1\right) + f\frac{SV_m}{S_f V_i} \right]. \quad (18)$$

As given by Kays and London [2], the friction factors are evaluated using Reynold's numbers of the fluids obtained from thermal analysis. The entrance and exit losses are not accounted for while investigating the pressure drops in this analysis. The elemental exchanger core outlet pressures are evaluated for models A1–A3 and tabulated in Tables 4–6. It can be seen from these tables that there is a significant variation in pressure drop due to flow nonuniformity, as there are considerable variations in velocities. For example, the maximum pressure drop values are: 17 times (for model A1), six times (for model A2) and two times (for model A3) higher when compared with uniform flow cases. The pressure drop for uniform flow case is 4.8 kPa with the inlet pressure of 100 kPa. The pumping power required is much higher for the flow nonuniformity case than the uniform flow case. It is recommended by Shah [8] that the core pressure drop be evaluated based on the highest velocity component of the flow maldistribution.

CONCLUSIONS

The thermal performance deteriorations and pressure drop variations of crossflow compact plate–fin heat exchangers have been reviewed with the effects

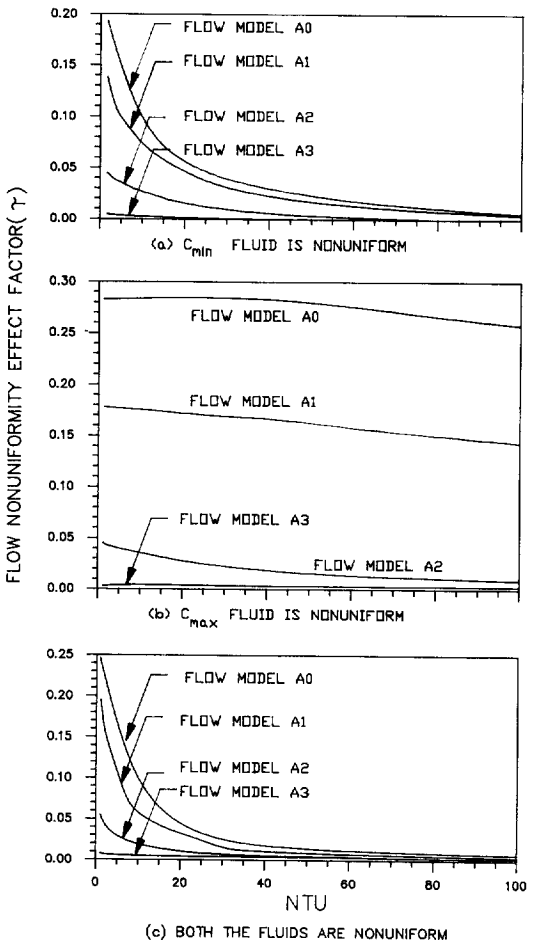

Fig. 6. Flow nonuniformity effects—$C_{min}/C_{max} = 0.4$.

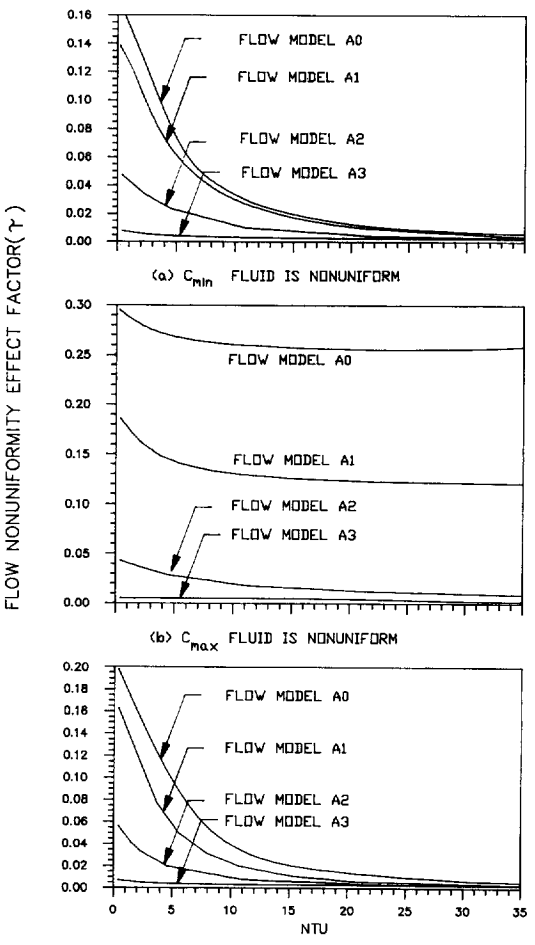

Fig. 7. Flow nonuniformity effects—$C_{min}/C_{max} = 0.2$.

of flow maldistribution. A mathematical equation has been developed to generate different types of fluid flow maldistribution models considering the possible deviations in fluid flow. This equation was found to be relevant in the generation of flow maldistribution models for a cross flow heat exchanger. Using these fluid flow maldistribution models, the exchanger effectiveness and its deteriorations due to flow non-uniformity are calculated on both the cold and hot fluid sides of an exchanger core for both balanced and unbalanced flows, and for the entire range of design and operating conditions. The results obtained, however, are not limited to proposed models and can also be interpolated/extrapolated to any other similar flow maldistribution models as well. In addition to

Table 4. Exchanger outlet pressure variations in model A1

$I=$	1	2	3	4	5	6	7	8	9	10
J										
1	99.97	99.97	99.97	99.97	99.97	99.97	99.97	99.97	99.97	99.97
2	99.97	99.33	97.98	96.23	94.60	94.29	95.56	97.39	99.06	99.97
3	99.97	98.05	93.16	85.96	78.63	77.18	82.98	90.69	97.06	99.97
4	99.97	96.52	86.76	70.79	51.76	47.84	64.25	81.86	94.69	99.97
5	99.97	95.29	81.17	55.36	19.20	19.00	43.89	74.15	92.78	99.97
6	99.97	95.29	81.17	55.36	19.20	19.00	43.89	74.15	92.78	99.97
7	99.97	96.52	86.76	70.79	51.76	47.84	64.25	81.86	94.69	99.97
8	99.97	98.05	93.16	85.96	78.63	77.18	82.98	90.69	97.06	99.97
9	99.97	99.33	97.98	96.23	94.60	94.29	95.56	97.39	99.06	99.97
10	99.97	99.97	99.97	99.97	99.97	99.97	99.97	99.97	99.97	99.97

Conditions: (a) inlet pressure = 100 kPa; (b) outlet pressure (if flow is uniform) = 95.17 kPa; (c) NTU = 8.0, $C_{min}/C_{max} = 1.0$ and $(\theta ha)_h/(\theta ha)_c = 1.0$.

Table 5. Exchanger outlet pressure variations in model A2

$I=$	1	2	3	4	5	6	7	8	9	10
J										
1	99.00	98.90	98.90	98.90	98.85	98.81	98.80	98.75	98.70	98.70
2	99.00	98.07	96.88	95.63	94.56	94.29	94.95	96.05	97.35	98.54
3	99.00	97.03	94.02	90.46	87.26	86.54	88.77	92.20	95.75	98.47
4	99.00	96.05	90.99	84.57	78.55	77.29	81.75	88.15	94.26	98.43
5	99.00	95.33	88.64	79.78	71.10	69.37	76.02	85.01	93.17	98.42
6	99.00	95.33	88.64	79.78	71.11	69.37	76.02	85.01	93.17	98.42
7	99.00	96.05	90.99	84.57	78.55	77.29	81.75	88.15	94.26	98.43
8	99.00	97.03	94.02	90.46	87.26	86.54	88.77	92.20	95.75	98.47
9	99.00	98.07	96.88	95.63	94.56	94.29	94.95	96.05	97.35	98.54
10	99.00	98.90	98.90	98.90	98.85	98.81	98.80	98.75	98.70	98.70

Conditions: (a) inlet pressure = 100 kPa; (b) outlet pressure (if flow is uniform) = 95.17 kPa; (c) NTU = 8.0, $C_{min}/C_{max} = 1.0$ and $(\theta ha)_h/(\theta ha)_c = 1.0$.

Table 6. Exchanger outlet pressure variations in model A3

$I=$	1	2	3	4	5	6	7	8	9	10
J										
1	96.61	96.38	96.16	96.00	96.00	95.60	95.43	95.29	95.18	95.06
2	96.61	96.00	95.41	94.89	94.45	94.21	94.19	94.33	94.61	95.00
3	99.61	95.69	94.73	93.86	93.14	92.83	92.99	93.44	94.13	94.96
4	99.61	95.45	94.19	92.99	92.02	91.65	91.98	92.73	93.77	94.93
5	99.61	95.29	93.83	92.41	91.26	90.86	91.30	92.25	93.53	94.91
6	99.61	95.29	93.83	92.41	91.26	90.86	91.30	92.25	93.53	94.91
7	99.61	95.45	94.19	92.99	92.02	91.65	91.98	92.73	93.77	94.93
8	99.61	95.69	94.73	93.86	93.14	92.83	92.99	93.44	94.13	94.96
9	99.61	96.00	95.41	94.89	94.45	94.21	94.19	94.33	94.61	95.00
10	99.61	96.38	96.16	96.00	96.00	95.60	95.43	95.29	95.18	95.06

Conditions: (a) inlet pressure = 100 kPa; (b) outlet pressure (if flow is uniform) = 95.17 kPa; (c) NTU = 8.0, $C_{min}/C_{max} = 1.0$ and $(\theta ha)_h/(\theta ha)_c = 1.0$.

thermal analysis, the pressure drops and their deviations are also calculated for these models. The finite element model, introduced in this paper for the simple crossflow heat exchanger, predicts thermal performance deteriorations and pressure drop variations which are in good agreement with the available numerical solutions.

The information obtained in this study clearly indicates that the thermal performance deterioration and variation in pressure drops due to flow nonuniformity may become quite significant in some typical applications. This deterioration in thermal performance should not be ignored in the analysis, design and sizing of a heat exchanger. The information presented in this paper can provide the designer with a means of estimation of effective performance deterioration when fluid flow is not uniformly distributed about an exchanger core. This estimation can reduce the number of tests and modifications of the prototype to a minimum for similar applications.

Acknowledgements—The authors are grateful to Professor S. K. Lakshmana Rao (retired), Regional Engineering College, Warangal, India for his valuable guidance in developing a mathematical equation for fluid flow nonuniformity models while carrying out this work. The authors are grateful to Dr R. K. Shah, Harrison Division, General Motors Corporation, New York, U.S.A. for the useful suggestions, during his visit to India in 1991, in carrying out this work.

REFERENCES

1. J. P. Holman, *Heat Transfer* (4th Edn), Chap. 10. McGraw-Hill, New York (1981).
2. W. M. Kays and A. L. London, *Compact Heat Exchangers* (3rd Edn). McGraw-Hill, New York (1984).
3. J. P. Chiou, The advancement of compact heat exchanger theory considering the effects of longitudinal heat conduction and flow nonuniformity effects. In *Compact Heat Exchangers—History, Technological Advancement and Mechanical Design Problems* (Edited by R. K. Shah, A. D. Kraus and D. Metyger), pp. 101–121. ASME, New York (1980).
4. J. P. Chiou, Thermal performance deterioration in a crossflow heat exchanger due to the flow nonuniformity, *J. Heat Transfer Trans. ASME* **100**, 580–587 (1978).
5. J. P. Chiou, The effect of air flow nonuniformity on the thermal performance of an automobile air conditioning condenser, *SAE Transaction*, no. 830542, pp. 2.587–2.600 (1984).
6. J. P. Chiou, The effect of air flow nonuniformity on the thermal performance of an evaporator of automobile air conditioning system, *SAE Transaction*, no. 840381, pp. 2.991–2.1005 (1985).
7. J. P. Chiou, Thermal performance deterioration in a crossflow heat exchanger due to the flow nonuniformity on both hot and cold sides, *Sixth International Heat Transfer Conference*, Vol. 4, pp. 279–284 (1978).

8. R. K. Shah, Flow maldistribution—compact heat exchangers. In *Handbook of Heat Transfer Applications* (Edited by W. M. Rohsenow, P. J. Hartnett and E. N. Ganić), pp. 266–280. McGraw-Hill, New York (1985).
9. R. K. Shah and A. L. London, Effects of nonuniform passages on compact heat exchanger performance, *J. Engng Power Trans. ASME* **102,** 653–659 (1980).
10. R. K. Shah and A. L. London, Influence of brazing on very compact heat exchanger surfaces, ASME paper 71-HT-29 (1971).
11. A. C. Mueller and J. P. Chiou, Review of various types of flow maldistribution in heat exchangers, *Heat Transfer Engng* **9,** 36–50 (1988).
12. R. B. Fleming, The effect of flow distribution in parallel channels of counterflow heat exchangers, *Adv. Cryogenic Engng* **12,** 352–361 (1966).
13. E. M. Sparrow and Y. S. Berman, Heat exchanger situated downstream of a right-angle bend, *Int. J. Heat Mass Transfer* **27,** 1649–1657 (1984).
14. Y. Hayashi and E. Hirai, Effect of maldistribution fluid on the performance of crossflow dry-cooling towers, *J. Chem. Engng Jap.* **17,** 286–293 (1984).
15. S. C. Kranc, The effect of nonuniform water distribution on cooling tower performance, *J. Energy* **7,** 636–639 (1983).
16. S. G. Ravikumar, K. N. Seetharamu and P. A. Aswatha Narayana, Performance evaluation of crossflow compact heat exchangers using finite elements, *Int. J. Heat Mass Transfer* **32,** 889–894 (1989).
17. S. G. Ravikumar, K. N. Seetharamu and P. A. Aswatha Narayana, Analysis of compact heat exchangers using finite element method. In *Heat Transfer*, Vol. 2, pp. 379–384. Hemisphere, New York (1986).
18. H. Yamasheta, R. Izumi and S. Yamaguchi, Performance of cross flow heat exchangers with variable physical properties, *Bull. JSME* **20,** 1008–1015 (1977).
19. L. J. Segerlind, *Applied Finite Element Analysis* (2nd Edn). Wiley, New York (1982).
20. B. S. Baclic, A simplified formula for crossflow heat exchanger effectiveness, *J. Heat Transfer Trans. ASME* **100,** 746–747 (1978).
21. B. S. Baclic and P. J. Heggs, On the search for new solutions of the single-pass crossflow heat exchanger problem, *Int. J. Heat Mass Transfer* **28,** 1965–1976 (1985).